# Synthesis and Characterization of Novel 2-Amino-3-benzoylthiophene Derivatives as Biased Allosteric Agonists and Modulators of the Adenosine A₁ Receptor

Celine Valant,[†] Luigi Aurelio,[‡] Shane M. Devine,[‡] Trent D. Ashton,[‡] Jonathan M. White,[§] Patrick M. Sexton,[†] Arthur Christopoulos,*,[†] and Peter J. Scammells*,[‡]

[†]Drug Discovery Biology and Department of Pharmacology and [‡]Medicinal Chemistry, Monash Institute of Pharmaceutical Sciences, Monash University, 381 Royal Parade, Parkville VIC 3052, Australia

[§]School of Chemistry and the Bio21 Molecular Science and Biotechnology Institute, The University of Melbourne, Melbourne VIC 3010, Australia

ABSTRACT: A series of novel 2-amino-3-benzoylthiophenes (2A3BTs) were screened using a functional assay of A₁R mediated phosphorylation of extracellular signal-regulated kinases 1 and 2 (ERK1/2) in intact CHO cells to identify potential agonistic effects as well as the ability to allosterically modulate the activity of the orthosteric agonist, *R*-PIA. Two derivatives, **8h** and **8i**, differing only in terms of the absence or presence of an electron-withdrawing group on the benzoyl moiety of the 2A3BT scaffold, were identified as biased allosteric agonists and positive allosteric modulators of agonist function at the adenosine A₁ receptor (A₁R) in two different functional assays. Our findings indicate that subtle structural variations can promote functionally distinct receptor conformational states.
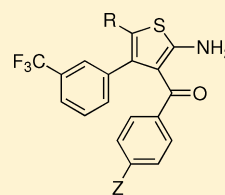
8h R = CH₃, Z = H
8i R = CH₃, Z = Cl

INTRODUCTION

G protein-coupled receptors (GPCRs) are the largest single class of drug targets,[1] and it is now well recognized that most, if not all, GPCRs possess topographically distinct allosteric binding sites that present attractive opportunities for the development of more targeted therapeutics.[2−5] The A₁R was one of the first GPCRs for which positive allosteric modulators of agonist function were described.[6,7] Despite the early identification of the 2A3BT scaffold as a key feature of allosteric modulators of A₁R and the numerous structure–activity relationships (SAR) subsequently disclosed, improvements in the potency and degree of positive allosteric modulation over and above the original series described by Bruns and colleagues have been relatively modest.[8−17]

An alternative approach to achieving selectivity of signaling at GPCRs is to pursue ligands that preferentially stabilize distinct subsets of receptor conformations to the relative exclusion of others. This phenomenon has been dubbed "stimulus bias" or "functional selectivity"[18,19] and is associated with ligand-directed signaling outcomes manifested as changes in rank orders of potency and or maximal effects relative to a reference (e.g., the endogenous) agonist. Allosteric modulators may impose stimulus bias in the actions of orthosteric ligands by differentially modulating some pathways relative to others. Indeed, we have demonstrated this to be the case with the 2A3BTs compounds **1** and **2** (Figure 1A), which differentially modulated the effects of the orthosteric agonist, *R*-PIA, in mediating ERK1/2 phosphorylation (pERK1/2) relative to [³⁵S]GTPγS binding to activated G proteins.[15] Interestingly, many 2A3BTs that show some degree of allosteric potentiation of A₁R agonist function also display direct agonist properties on their own (i.e., in the absence of orthosteric ligand), suggesting

that these compounds are able to stabilize A₁Rs in more than one active state and may thus promote stimulus bias even in the absence of orthosteric agonist.[6,20,21] For example, we recently found that the well-characterized 2A3BT, T62 (**3**), as well as two novel modulators/agonists, VCP520 (**4**) and VCP333 (**5**) (Figure 1B), exhibited stimulus bias toward cAMP inhibition compared to pERK1/2, whereas the orthosteric agonist, *R*-PIA, was strongly biased toward the latter pathway.

In both cases, the compounds under comparison possessed a 2-amino group and the same substituent in the 3-position [3-benzoyl group or 3-(4-chlorobenzoyl)], with the point of divergence being in the 4/5 positions of the thiophene core. However, in numerous earlier studies, the nature of the 3-benzoyl group has been shown to have a profound effect on allosteric activity. Examples of substituents that impart favorable activity include the 3-(3-trifluoromethyl)benzoyl present in PD81,723, the 3-(3,4-dichlorobenzoyl) in LUF 5484 as well as the 3-(4-chlorobenzoyl) in T62.[7,8] Most recently, we have shown that an analogue of T62 with a 3-(4-methylbenzoyl) substituent acted as both an allosteric enhancer and an allosteric agonist. Herein, we report our investigations on the influence of further substitution on the 3-benzoyl group of allosteric modulation and biased signaling. More specifically, we have targeted analogues of compounds **1** and **2** that possess a 4-phenyl with electronegative substituents, namely (3-trifluoromethyl) or 4-(3,5-bistrifluoromethyl), as this has proven to be an important feature for engendering intrinsic agonist activity. A test set of the most interesting 3-benzoyl groups from previous studies (i.e., 4-Cl, 3,4-Cl, 3-CF₃, and 4-
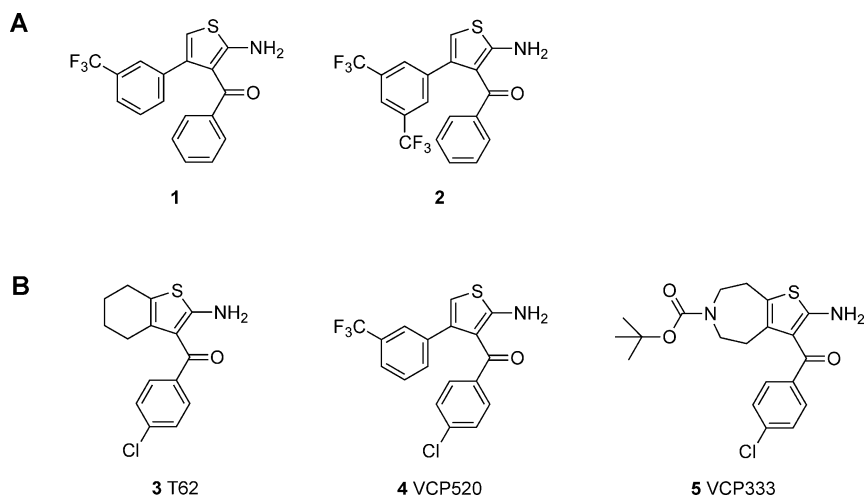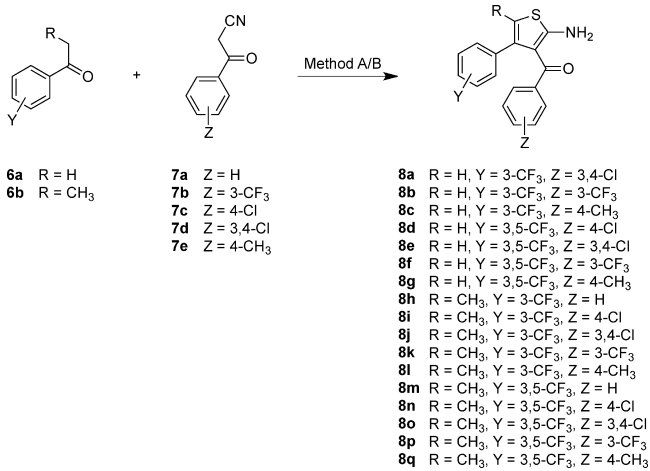
Figure 1. Structure of allosteric ligands mentioned in this study. (A) Allosteric modulators that imposed biased signaling in the actions of the orthosteric agonist, R-PIA.[21] (B) Previously characterized A_1R allosteric modulators that promote stimulus bias in the absence of orthosteric agonist.[21]

Me) has been used to probe the influence of this group on allosteric activity and downstream cell signaling. We find that even simple substitutions can lead to marked changes in the signaling bias of the A_1R when occupied by allosteric agonists alone and in the presence of a cobound orthosteric agonist.

■ RESULTS AND DISCUSSION

Chemistry. The synthesis of the 2-amino-3-benzoylthiophenes **8a–q** was performed via either a two-step or one-pot microwave-assisted Gewald procedure (Scheme 1). The two-

Scheme 1[a]

6a R = H	**7a** Z = H	**8a** R = H, Y = 3-CF$_3$, Z = 3,4-Cl			
6b R = CH$_3$	**7b** Z = 3-CF$_3$	**8b** R = H, Y = 3-CF$_3$, Z = 3-CF$_3$			
	7c Z = 4-Cl	**8c** R = H, Y = 3-CF$_3$, Z = 4-CH$_3$			
	7d Z = 3,4-Cl	**8d** R = H, Y = 3,5-CF$_3$, Z = 4-Cl			
	7e Z = 4-CH$_3$	**8e** R = H, Y = 3,5-CF$_3$, Z = 3,4-Cl			

8a R = H, Y = 3-CF$_3$, Z = 3,4-Cl
8b R = H, Y = 3-CF$_3$, Z = 3-CF$_3$
8c R = H, Y = 3-CF$_3$, Z = 4-CH$_3$
8d R = H, Y = 3,5-CF$_3$, Z = 4-Cl
8e R = H, Y = 3,5-CF$_3$, Z = 3,4-Cl
8f R = H, Y = 3,5-CF$_3$, Z = 3-CF$_3$
8g R = H, Y = 3,5-CF$_3$, Z = 4-CH$_3$
8h R = CH$_3$, Y = 3-CF$_3$, Z = H
8i R = CH$_3$, Y = 3-CF$_3$, Z = 4-Cl
8j R = CH$_3$, Y = 3-CF$_3$, Z = 3,4-Cl
8k R = CH$_3$, Y = 3-CF$_3$, Z = 3-CF$_3$
8l R = CH$_3$, Y = 3-CF$_3$, Z = 4-CH$_3$
8m R = CH$_3$, Y = 3,5-CF$_3$, Z = H
8n R = CH$_3$, Y = 3,5-CF$_3$, Z = 4-Cl
8o R = CH$_3$, Y = 3,5-CF$_3$, Z = 3,4-Cl
8p R = CH$_3$, Y = 3,5-CF$_3$, Z = 3-CF$_3$
8q R = CH$_3$, Y = 3,5-CF$_3$, Z = 4-CH$_3$

[a]Method A: (i) CH$_2$Cl$_2$, TiCl$_4$, pyridine; (ii) THF, S$_8$, Et$_2$NH. Method B: S$_8$, Et$_2$NH, microwave.

step approach (method A) initially involved a titanium(IV) chloride mediated Knoevenagel condensation to give an intermediate alkene that subsequently underwent ring closing under basic conditions in the presence of elemental sulfur to furnish the desired 2A3BTs. In the one-pot procedure (method B), the benzoylacetonitrile, acetophenone or propiophenone, sulfur, and base (Et$_2$NH) were heated at 130 °C for 1 h in a microwave reactor. In both cases, the crude thiophenes were purified via silica gel chromatography.

Interestingly, compound **8h** was found to dimerize upon standing in CDCl$_3$. The structure of the dimer was confirmed by X-ray crystallography (Figure 2). This dimerization resulted
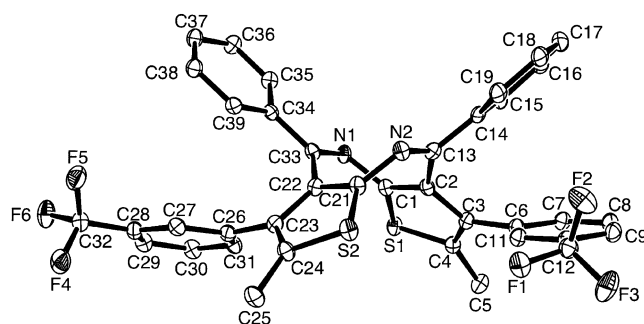
Figure 2. A thermal ellipsoid plot for the dimer **8h**. The 8-membered ring adopts a tub conformation, with a local 2-fold axis of symmetry orthogonal to the plane defined by the atoms N1, N2, C13, and C33 in the 8-membered ring, the 2-fold symmetry is broken only by the orientations of the trifluoromethylphenyl substituents.

from the condensation of the 2-amino moiety of one molecule with the 3-benzoyl group of another. We have only previously observed dimerization of this type under acidic conditions (refluxing in 0.5 M HCl for 7 h).[22] A stability study was conducted in order to determine if this dimerization might be occurring in DMSO stock solutions upon storage. However, **8h** was found to be stable in DMSO (over a 4 week period), which suggested that the dimerization observed previously was promoted by traces of acid in the CDCl$_3$.

Pharmacology. To assess the biological activity of the novel series of compounds, we initially screened all compounds using a plate-based assay of A_1R-mediated pERK1/2 in intact CHO cells.[14−17] For each compound, two concentrations (3 and 10 μM) were tested alone to assess intrinsic agonism, and against an EC$_{50}$ concentration of the orthosteric agonist R-PIA, to assess enhancement or inhibition of the A_1R agonist activity. Most compounds, being analogues of **1** and **2**, displayed a high degree of agonism on their own, as indicated in Figure 3A. It has already been observed previously that the presence of a 3-trifluoromethyl or 3,5-bis(trifluoromethyl) group on the phenyl in the 4-position of the thiophene ring induces strong agonist

A

B
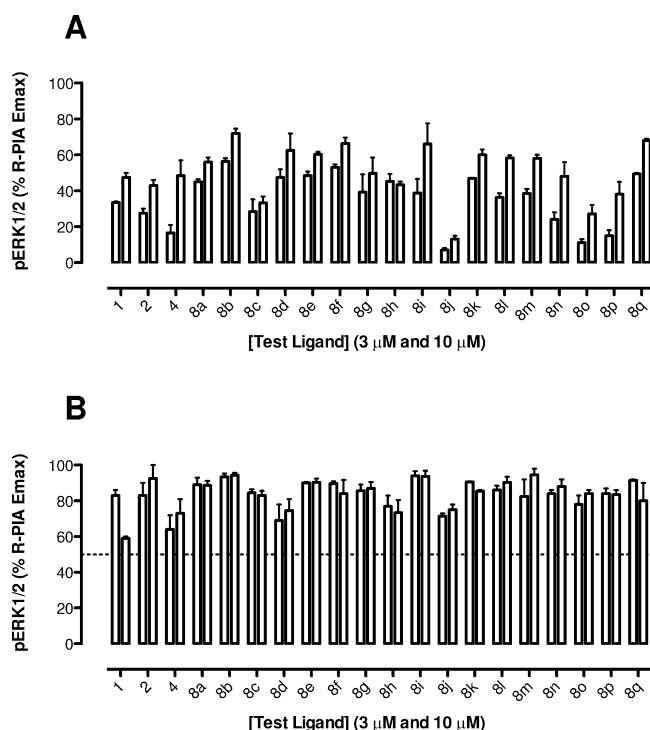
Figure 3. Effect of two different concentrations (3 μM, white bar; 10 μM, black bar) of novel 2-amino-3-benzoylthiophenes on A_1R-mediated stimulation of ERK1/2 phosphorylation in intact CHO FlpIn cells, in absence (A) or presence (B) of an EC_{50} concentration of R-PIA (determined on the same day as each assay). Data represent the mean ± standard deviation of two to three experiments conducted in triplicate.

properties of the 2A3BT derivatives.[15] The capacity of these compounds to potentiate R-PIA and A_1R-mediated ERK1/2 phosphorylation was also screened at two concentrations (3 and 10 μM) (Figure 3B and Table 1). Pleasingly, the combination of substituents known to promote allosteric activity in the 3- and 4-positions afforded a series of compounds that demonstrated substantial functional potentiation of R-PIA/A_1R mediated increases in ERK1/2 phosphorylation. Even at the lowest test concentration (3 μM), 13 of the 17 new 2A3BTs afforded greater than 80% of the maximum attainable R-PIA response by a concentration of agonist that normally yields 50% of the maximal response. Five of these compounds produced over 90% of the maximum attainable R-PIA response at this concentration (Table 1).

To further investigate the results of this initial screen, more detailed experiments were performed using the most efficacious allosteric modulator identified in this series of compounds, **8i**, as well as its closest analogue, **8h**, differing only in terms of the absence of an electron-withdrawing group, 4-Cl, on the benzoyl moiety of the 2A3BT scaffold. The biological activity of these two 2A3BT derivatives was assessed in both pERK1/2 and cAMP inhibition assays performed in recombinant CHO-FlpIn cells stably expressing the human A_1R. As shown in parts A and B of Figure 4, increasing concentrations of either compound caused a significant enhancement of the potency of R-PIA for mediating pERK1/2, indicative of positive allosteric modulation of the orthosteric agonist. Concomitantly, a substantial degree of R-PIA-independent receptor activation was also noted for both novel 2A3BT derivatives, as previously observed in the initial functional screen, indicating that they were allosteric

agonists for the pERK1/2 pathway in their own right. At the level of cAMP inhibition (Figure 4C,D), both 2A3BTs again enhanced the potency of the orthosteric agonist, R-PIA, but only **8h** retained appreciable allosteric agonist activity.

To quantify these properties, we applied an operational model of agonism and allosterism to the data to derive estimates of the following three parameters: the affinity of each modulator for the allosteric site on the unoccupied A_1R (quantified as the negative logarithm of the dissociation constant, pK_B), a measure of the operational efficacy of each modulator at the A_1R (quantified as the logarithm, $\log\tau_B$), and a measure of the cooperativity of each modulator on R-PIA potency (quantified as a logarithm of the composite cooperative effects on both binding affinity and signaling efficacy, $\log\alpha\beta$). The results of this analysis are shown in Table 2.

For compound **8h**, the affinity estimates were similar between pERK1/2 and cAMP assays but significantly higher than the pK_B values estimated for **8i** at the corresponding pathways (Table 2). This suggests that the presence of the 4-Cl on the benzoyl group of the 2A3BT scaffold was detrimental to the interaction of the ligand with the allosteric binding site in the A_1R. In terms of the magnitude of the allosteric effect of each 2A3BT on R-PIA signaling, **8h** exhibited similar degrees of cooperativity with R-PIA between pERK1/2 ($\alpha\beta$ = 4.1) and cAMP inhibition ($\alpha\beta$ = 3.2), while the values for the effect of **8i** were higher, $\alpha\beta$ = 12 and $\alpha\beta$ = 18 for pERK1/2 and cAMP inhibition, respectively. This suggests that the presence of a 4-chloro on the benzoyl group of the 2A3BT scaffold increases the allosteric interaction with R-PIA, even though it reduces the affinity of the modulator at the A_1R. It also highlights the fact that these two parameters are not correlated, thus justifying why they should be separately determined in order to better understand underlying SAR of allosteric ligands.

When comparing the intrinsic agonist properties of each of the allosteric ligands, **8h** exhibited similar efficacy values for pERK1/2 (τ_B = 0.63) and cAMP (τ_B = 0.59), whereas **8i** showed greater efficacy in pERK1/2 (τ_B = 2.0) than cAMP inhibition (τ_B = 0.06). Given that the potency (as defined by the EC_{50}) of the prototypical orthosteric agonist, R-PIA, is 100-fold greater for signaling to pERK1/2 (pEC_{50} = 9.64 ± 0.04) relative to cAMP inhibition (pEC_{50} = 7.73 ± 0.03), the lack of change in the efficacy of **8h** between the same two pathways is particularly striking and indicative that the allosteric agonist is biased relative to the orthosteric agonist. This is more evident in Figure 5A, where the percentage responses to equimolar concentrations of each agonist between the two pathways are plotted against each other in the form of a "bias plot".[21,23] For comparative purposes, we also generated the bias plot for our previously published compound **4**,[15] which demonstrated an even more marked bias toward cAMP accumulation over ERK1/2 phosphorylation than that of **8h**. In contrast, **8i** followed the pathway preferences of R-PIA, suggesting that this allosteric agonist is not biased relative to the orthosteric agonist. This does not mean that either of these latter agents are "non-biased", only that their coupling preferences are distinct from those of **8h**.

To statistically quantify the bias of our 2A3BT derivatives compared to R-PIA, we determined "bias factors" for each of the agonists using a method based on the operational model of agonism; see Experimental Section. Specifically, we have shown previously[24,25] that the ratio of τ_B/K_B for a given agonist at a signal pathway (referred to as the "transduction ratio", TR),

Table 1. Effect of Test Compounds on A_1R-Mediated Stimulation of ERK1/2 Phosphorylation in Intact CHO Cells in the Presence of an EC_{50} Concentration of R-PIA
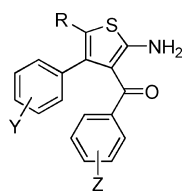
|	structure			activity		
	R	Y	Z	3 μM	10 μM	n
1[15]	H	3-CF$_3$	H	83 ± 3	59 ± 1	2
4[15]	H	3-CF$_3$	4-Cl	64 ± 8	73 ± 8	2
8a	H	3-CF$_3$	3,4-Cl	88 ± 6	88 ± 5	2
8b	H	3-CF$_3$	3-CF$_3$	93 ± 2	94 ± 2	3
8c	H	3-CF$_3$	4-CH$_3$	85 ± 2	83 ± 3	3
2[15]	H	3,5-CF$_3$	H	83 ± 7	93 ± 8	2
8d	H	3,5-CF$_3$	4-Cl	69 ± 9	74 ± 7	2
8e	H	3,5-CF$_3$	3,4-Cl	90 ± 1	90 ± 2	3
8f	H	3,5-CF$_3$	3-CF$_3$	90 ± 2	84 ± 8	3
8g	H	3,5-CF$_3$	4-CH$_3$	86 ± 4	87 ± 4	3
8h	CH$_3$	3-CF$_3$	H	77 ± 6	73 ± 3	3
8i	CH$_3$	3-CF$_3$	4-Cl	94 ± 3	94 ± 4	3
8j	CH$_3$	3-CF$_3$	3,4-Cl	73 ± 3	75 ± 3	2
8k	CH$_3$	3-CF$_3$	3-CF$_3$	90 ± 1	86 ± 1	2
8l	CH$_3$	3-CF$_3$	4-CH$_3$	86 ± 3	90 ± 3	3
8m	CH$_3$	3,5-CF$_3$	H	83 ± 9	95 ± 3	2
8n	CH$_3$	3,5-CF$_3$	4-Cl	84 ± 2	88 ± 4	2
8o	CH$_3$	3,5-CF$_3$	3,4-Cl	78 ± 5	84 ± 2	2
8p	CH$_3$	3,5-CF$_3$	3-CF$_3$	84 ± 3	84 ± 3	2
8q	CH$_3$	3,5-CF$_3$	4-CH$_3$	92 ± 1	80 ± 10	2

once normalized to that of a reference agonist, can be used to derive a bias factor as a quantitative measure of signal pathway bias. If the test agonist (i.e., allosteric ligand) and reference agonist (i.e., R-PIA) activate the two pathways via a common receptor conformation, the bias factor should be 1.0, irrespective of differences in response amplification between pathways. In contrast, significant deviation of the bias factors from 1.0 indicates the involvement of distinct conformations for the different agonists in mediating the various pathways. As shown in Table 3 and Figure 5B, **8h** displayed a significant 45-fold bias toward cAMP relative to pERK1/2 when compared to the signaling preferences of R-PIA; in contrast, the bias toward cAMP signaling of **8i** was only 3.5-fold. This is not to say the R-PIA and **8i** do not display signaling bias, but for the pathways studied herein, their coupling preferences individually at the A_1R track with one another, whereas those of **8h** clearly diverge. Collectively, these results suggest that the nature of the binding locus used by the different ligands, i.e., orthosteric versus allosteric site, is unlikely to be the sole determinant of the ability of a given agonist to engender stimulus-bias.

According to a simple two-state model of receptor activation, it would be expected that the degree of positive allosteric enhancement should correlate with the degree of direct allosteric agonism displayed by a given modulator.[26,27] The behavior of **8h** when combined with R-PIA is certainly in accord with this hypothesis, given that it displayed similar degrees of agonism (τ_B) and cooperativity ($\alpha\beta$) between

pERK1/2 and cAMP inhibition pathways. However, this does not hold for **8i** because it is clearly less efficacious at inhibiting cAMP relative to promoting pERK1/2 yet has similar robust positive cooperativities with R-PIA at both pathways; if anything, the positive cooperativity is greater at cAMP inhibition, the pathway associated with the least direct allosteric agonism (Table 2). This finding highlights two important points. First, it is necessary to postulate the existence of more than a single active receptor state to accommodate the data. Second, although **8i**, on its own, appears to bias receptor signaling in manner that is similar to that of R-PIA, the *cobinding* of the modulator and R-PIA to the A_1R promotes a functionally distinct state, an example of allosteric modulator-engendered functional selectivity.[26−29] In contrast, the opposite appears to be the case with **8h**, i.e., as an allosteric agonist, this compound is biased, but as an allosteric modulator of R-PIA, it retains similar preferences across pathways.

■ CONCLUSIONS

In summary, two novel 2A3BT derivatives, differing only with regards to the absence (**8h**) or presence (**8i**) of a halogen atom in the 4-position of the benzoylthiophene ring, promote functionally biased states of the adenosine A_1R. In comparison to the orthosteric agonist, R-PIA, **8h** (alone) was biased as an allosteric agonist toward cAMP accumulation over ERK1/2 phosphorylation, whereas **8i** showed minimal bias. In contrast, when combined with R-PIA, **8h** allosterically modulated the
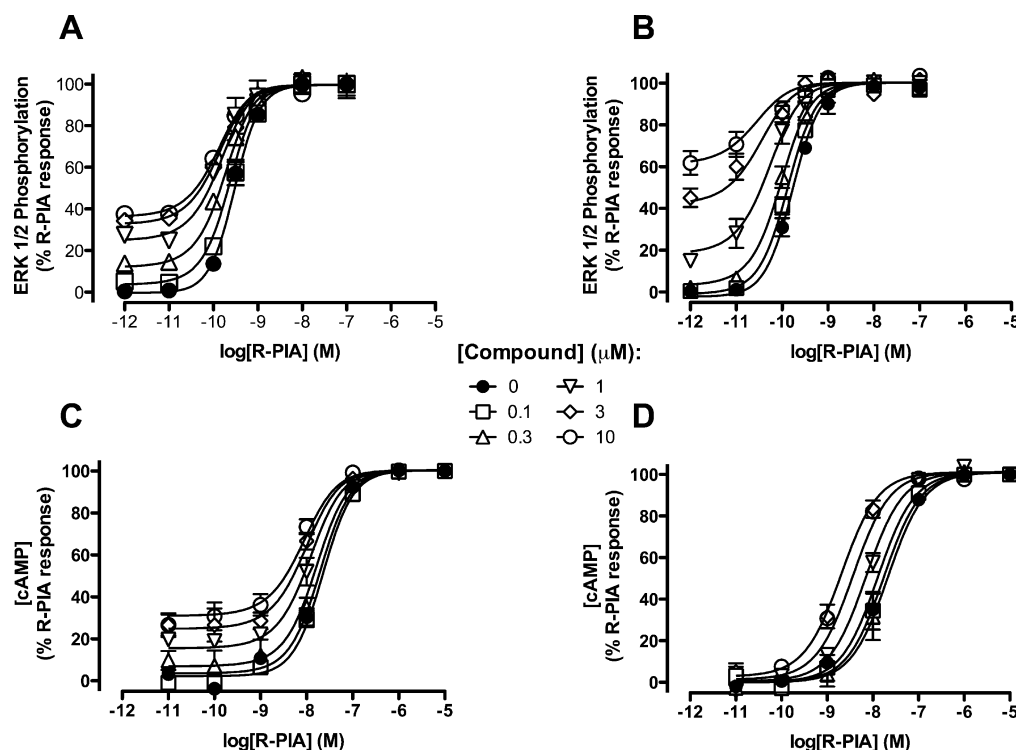
Figure 4. Positive allosteric modulation of *R*-PIA-mediated response by 2A3BTs. Effects of **8h** (A,C) or **8i** (B,D) on *R*-PIA-mediated ERK1/2 phosphorylation (A−B), or cAMP inhibition (C−D). Data points represent the mean ± SE obtained from three to five experiments conducted in duplicate. Curves drawn through the data represent the fit of an operational model of allosterism.

Table 2. Operational Model Parameters for the Functional Allosteric Interaction between *R*-PIA and Modulators at the A_1R (Parameter Values Represent the Mean ± SEM from Three Experiments Performed in Duplicate)

|	Compound 8h		Compound 8i	
	pERK1/2	cAMP inhibition	pERK1/2	cAMP inhibition
pK_b [a]	6.16 ± 0.10	5.87 ± 0.12	5.37 ± 0.14	5.14 ± 0.22
$Log\tau_B$ (τ_B) [b]	−0.20 ± 0.05 (0.63)	−0.23 ± 0.05 (0.59)	0.31 ± 0.07 (2.0)	-1.20 ± 0.44 (0.06)
$Log\alpha\beta$ $(\alpha\beta)$ [c]	0.61 ± 0.07 (4.1)	0.50 ± 0.09 (3.2)	1.08 ± 0.15 (12)	1.25 ± 0.14 (18)

[a]Negative logarithm of the equilibrium dissociation constant of modulators (pK_b). [b]Logarithm of the operational efficacy parameter of the 2A3BTs as allosteric agonists. Antilogarithm shown in parentheses. [c]Logarithm of the product of the binding (α) and activation (β) cooperativity factors between *R*-PIA and modulators. Antilogarithm shown in parentheses.

activity of the orthosteric agonist at the two pathways in a nonbiased manner, whereas the combination of **8i** and *R*-PIA resulted in the generation of pathway-biased allosteric modulation. Collectively, these results highlight how a GPCR bound with both an allosteric modulator and an orthosteric agonist should be viewed as a unique protein state that differs from those promoted by either orthosteric or allosteric agonist alone. Furthermore, **8h** and **8i** represent novel tools with which to further probe the mechanistic basis of biased signaling at the A_1R.

■ EXPERIMENTAL SECTION

Chemistry. All reagents and anhydrous DMF were purchased from Aldrich and used without further purification. LR grade methanol, petroleum ether (40−60 °C), ethyl acetate, diethyl ether, and dichloromethane were purchased from Merck and were used without further purification. All microwave reactions were performed in a

Biotage Initiator microwave synthesizer. All ^{1}H NMR and ^{13}C NMR spectra were recorded on a Bruker Avance III 400 Ultrashield Plus spectrometer at 400.13 and 100.62 MHz, respectively. Thin-layer chromatography was conducted on 0.2 mm plates using Merck silica gel 60 F_{254}. Column chromatography was achieved using Merck silica gel 60 (particle size 0.063−0.200 μm, 70−230 mesh) and eluent percentages are described in volume (%v/v). High resolution mass spectra (HR-ESI) were obtained on a Waters LCT Premier XE (TOF) using electrospray ionization. Compound purity was analyzed on an Agilent 1200 series LCMS system employing a RP-HPLC Phenomenex column (Luna 5 μm C_8(2), 50 mm × 4.60 mm ID) at 30 °C, with a photodiode array detector (214/254 nm) coupled directly to an electrospray ionization source and a single quadrupole mass analyzer (Agilent 6120 Quadrupole MS). Chromatograms show UV absorbance at 254 nm. The following buffers were used; buffer A 99.9% H_2O, 0.1% formic acid; buffer B 99.9% CH_3CN, 0.1% formic acid. The following gradient was used with a flow rate of 0.5 mL/min and total run time of 12 min; 0−4 min 95% buffer A and 5% buffer B,
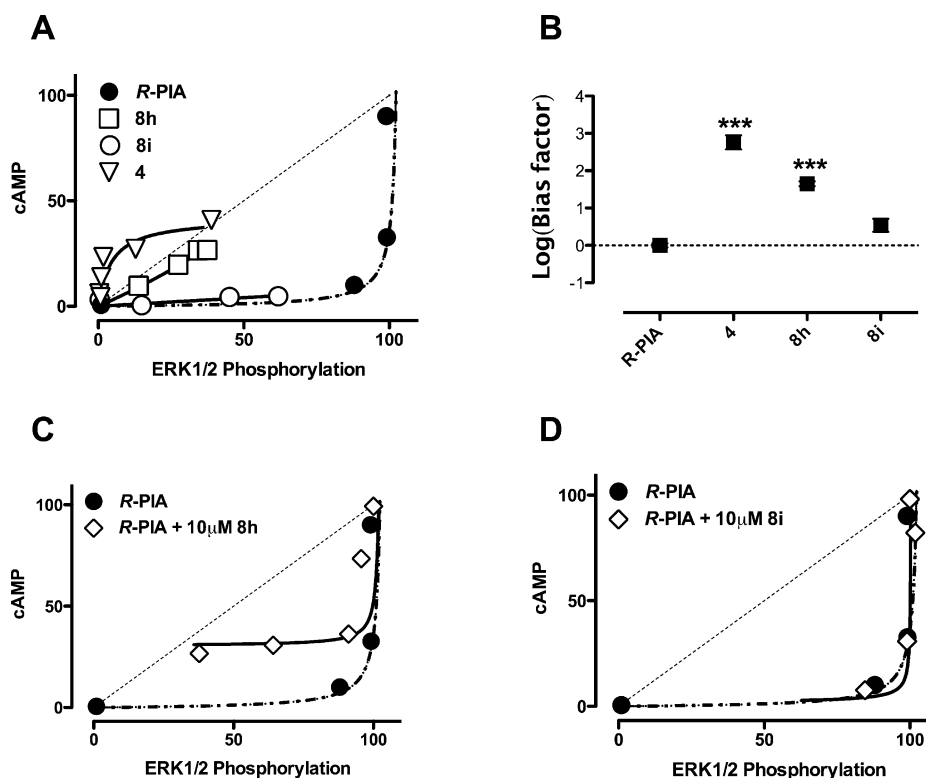
Figure 5. A_1R orthosteric and allosteric ligand signaling bias alone (A,B) or upon coadministration (C,D). (A,C,D) Bias plots of the responses corresponding to equimolar concentratons of the indicated ligands for ERK1/2 phosphorylation and cAMP inhibition assays. Data for compound **4** replotted from ref 21. (B) Bias factors, $\Delta\Delta\log(\tau/K_A)$, determined in both ERK1/2 phosphorylation and cAMP inhibition assays. *** indicates $P < 0.001$ relative to value for *R*-PIA.

Table 3. Estimation of Bias Factors for *R*-PIA and Selected 2A3BTs at the A_1R, Determined in Both ERK1/2 Phosphorylation and cAMP Inhibition Assays[a]

ligand	ERK1/2 phosphorylation		cAMP inhibition		LogBiasFactor [cAMP-pERK1/2] (bias factor)
	logTR	logTR$_n$	logTR	logTR$_n$	
R-PIA	9.55 ± 0.04	0.00 ± 0.06	7.71 ± 0.06	0.00 ± 0.08	0.00 ± 0.10 (1.00)
4	4.86 ± 0.29	-4.69 ± 0.29	5.78 ± 0.15	-1.93 ± 0.16	2.76 ± 0.33 (575)
8h	5.89 ± 0.04	-3.66 ± 0.05	5.70 ± 0.07	-2.01 ± 0.09	1.65 ± 0.11 (45)
8i	5.64 ± 0.03	-3.91 ± 0.05	4.34 ± 0.28	-3.37 ± 0.29	0.54 ± 0.30 (3.5)

[a]LogTR is the log of the "transduction ratio" (τ_A/K_A or τ_B/K_B), and logTR$_n$ values are normalized to the logTR for *R*-PIA. LogBF[cAMP-pERK1/2] represent the logarithm of the bias factor for cAMP inhibition pathway compared to pERK1/2 pathway; antilogarithms of the bias factor (BF) are shown in parentheses. Values represent the mean $\pm$ SEM from three experiments performed in duplicate. For compound **4**, these values were derived from our prior study.[21]

4−7 min 0% buffer A and 100% buffer B, 7−12 min 95% buffer A and 5% buffer B. Mass spectra were acquired in positive and negative ion mode with a scan range of 0−1000 m/z at 5 V. All compounds were of ≥95% purity.

General Procedure for the Synthesis of 8a−q. *Method A.* The acetophenone or propiophenone **6** (0.5 g, 2.47 mmol) and appropriate nitrile **7** (2.47 mmol) were dissolved in dry CH_2Cl_2 (16 mL) in an N_2 atmosphere and cooled to 0 °C with an ice bath. To the cooled solution was added neat titanium(IV) chloride (0.271 mL, 2.47 mmol) dropwise. After stirring on the ice bath for 0.5 h, pyridine (0.181 mL) was added dropwise and left to stir a further hour. Then another aliquot of pyridine (0.503 mL) was added dropwise and the ice bath removed, and the mixture was left to stir overnight. The mixture was diluted with CH_2Cl_2 (30 mL) and washed with 1 M HCl (30 mL). The organic was then washed with water (3 × 20 mL) and finally with brine (10 mL). The organic layer was dried ($MgSO_4$), filtered, and then concentrated to a resin that was taken up in THF (5 mL) and elemental sulfur (0.087 g, 2.71 mmol) was

added followed by diethylamine (0.654 mL) and stirred at room temperature for 5 h. The mixture was diluted with ether (40 mL) and washed with water (3 × 20 mL) and finally with brine (10 mL). The organic layer was dried ($MgSO_4$), filtered, and then concentrated to a resin that is chromatographed on silica gel with CH_2Cl_2.

Method B. The appropriate benzoylacetonitrile **7** (1.26 mmol) and appropriate acetophenone or propiophenone **6** (2.56 mmol, 2.0 equiv), S_8 (46 mg, 1.44 mmol, 1.1 equiv), and Et_2NH (26 μL, 0.25 mmol, 0.2 equiv) were heated at 130 °C for 1 h via microwave irradiation. The crude reaction mixture was purified by column chromatography using 4:1 petroleum spirits:EtOAc.

(2-Amino-4-(3-(trifluoromethyl)phenyl)thiophen-3-yl)(3,4-dichlorophenyl)methanone (8a). Method B. Compound **8a** was isolated as a yellow oil (181 mg, 31%). ^{1}H NMR (400 MHz, $CDCl_3$) δ 7.32−7.27 (m, 1H), 7.23−7.19 (m, 3H), 7.18−7.16 (m, 1H), 7.15 (dd, J = 8.2, 1.9 Hz, 1H), 7.09 (d, J = 8.2 Hz, 1H), 6.90 (s, 2H), 6.22 (s, 1H). ^{13}C NMR (101 MHz, $CDCl_3$) δ 189.7, 167.4, 139.8, 139.7, 137.9, 134.8, 131.8, 131.6 (d, J = 1.1 Hz), 130.9, 130.4 (q, J = 32.3 Hz),

129.8, 128.7, 127.61, 125.4 (q, *J* = 3.8 Hz), 123.8 (q, *J* = 272.6 Hz), 123.6 (q, *J* = 3.7 Hz), 114.3, 106.8. HR-ESMS calcd for $C_{18}H_{11}Cl_2F_3NOS^+$ (M + H) 415.9885, found 415.9878.

(2-Amino-4-(3-(trifluoromethyl)phenyl)thiophen-3-yl)(3-trifluoromethylphenyl)methanone (8b). Method A. Compound **8b** was isolated as a yellow oil (251 mg, 34%). ^{1}H NMR (400 MHz, CDCl₃) δ 7.53 (d, *J* = 7.7 Hz, 1H), 7.41 (s, 1H), 7.35 (dd, *J* = 7.8, 0.6 Hz, 1H), 7.22−7.08 (m, 5H), 6.96 (s, 2H), 6.22 (s, 1H). ^{13}C NMR (101 MHz, CDCl₃) δ 190.8, 167.5, 140.8, 139.9, 137.7, 131.7 (d, *J* = 0.9 Hz), 131.6 (d, *J* = 1.0 Hz), 130.3 (q, *J* = 32.3 Hz), 129.8 (q, *J* = 32.8 Hz), 128.6, 128.5, 127.1 (q, *J* = 3.6 Hz), 125.6 (q, *J* = 3.6 Hz), 125.5 (q, *J* = 3.6 Hz), 123.8 (q, *J* = 272.5 Hz), 123.6 (q, *J* = 272.5 Hz), 123.5 (q, *J* = 3.7 Hz), 114.2, 106.9. HR-ESMS calcd for $C_{19}H_{12}F_6NOS^+$ (M + H) 416.0538, found 416.0537.

(2-Amino-4-(3-(trifluoromethyl)phenyl)thiophen-3-yl)(p-tolyl)-methanone (8c). Method B. Compound **8c** was isolated as a yellow amorphous solid (109 mg, 16%) after recrystallization from a mixture of 2-propanol, water, and acetone. ^{1}H NMR (400 MHz, CDCl₃) δ 7.23−7.07 (m, 6H), 6.77 (d, *J* = 7.8 Hz, 2H), 6.61 (s, 2H), 6.22 (s, 1H), 2.15 (s, 3H). ^{13}C NMR (101 MHz, CDCl₃) δ 192.8, 165.7, 141.3, 140.6, 138.3, 137.2, 131.6 (d, *J* = 1.1 Hz), 130.1 (q, *J* = 32.2 Hz), 129.0, 128.3, 128.2, 125.6 (q, *J* = 3.9 Hz), 124.0 (q, *J* = 272.3 Hz), 123.0 (q, *J* = 3.8 Hz), 115.2, 106.4, 21.4. HR-ESMS calcd for $C_{19}H_{15}F_3NOS^+$ (M + H) 362.0821, found 362.0831.

(2-Amino-4-(3,5-bis(trifluoromethyl)phenyl)thiophen-3-yl)(4-chlorophenyl)methanone (8d).[15] Method A. Compound **8d** was isolated as a yellow solid. ^{1}H NMR (400 MHz, CDCl₃) δ 7.54 (bs, 1H), 7.42 (bs, 1H), 7.17 (d, *J* = 8.4 Hz, 2H), 6.97 (d, *J* = 8.4 Hz, 2H), 6.83 (bs, 2H), 6.31 (s, 1H). ^{13}C NMR (75.4 MHz, CDCl₃) δ 190.9, 167.0, 139.4, 139.3, 138.2, 137.1, 131.2 (q, *J* = 33.4 Hz), 129.9, 128.5, 127.9, 123.0 (q, *J* = 272.8 Hz), 120.2, 114.2, 107.6. HR-ESMS calcd for $C_{19}H_{11}ClF_6NOS^+$ (M + H) 450.0149, found 450.0163.

(2-Amino-4-(3,5-bis(trifluoromethyl)phenyl)thiophen-3-yl)(3,4-dichlorophenyl)methanone (8e). Method B. Compound **8e** was isolated as a yellow oil (159 mg, 23%). ^{1}H NMR (400 MHz, CDCl₃) δ 7.55 (s, 1H), 7.42 (s, 2H), 7.19−7.09 (m, 3H), 7.01 (s, 2H), 6.29 (s, 1H). ^{13}C NMR (101 MHz, CDCl₃) δ 189.3, 167.8, 139.5, 139.2, 138.2, 135.2, 132.1, 131.5 (q, *J* = 33.5 Hz), 130.8, 130.1, 128.4 (d, *J* = 2.7 Hz), 127.5, 123.0 (q, *J* = 272.9 Hz), 120.5 (dt, *J* = 7.5, 3.8 Hz), 113.9, 108.0. HR-ESMS calcd for $C_{20}H_9F_9NOS^-$ (M − H) 481.9613, found 481.9629.

(2-Amino-4-(3,5-bis(trifluoromethyl)phenyl)thiophen-3-yl)(3-trifluoromethylphenyl)methanone (8f). Method B. Compound **8f** was isolated as a yellow oil (81 mg, 12%). ^{1}H NMR (400 MHz, CDCl₃) δ 7.55 (d, *J* = 7.7 Hz, 1H), 7.46 (s, 1H), 7.43−7.35 (m, 4H), 7.25−7.19 (m, 1H), 6.98 (s, 2H), 6.31 (s, 1H). ^{13}C NMR (101 MHz, CDCl₃) δ 190.4, 167.7, 140.6, 139.0, 138.3, 131.7 (d, *J* = 0.7 Hz), 131.5 (q, *J* = 33.4 Hz), 130.2 (q, *J* = 33.2 Hz), 128.8, 128.4 (d, *J* = 2.7 Hz), 127.4 (q, *J* = 3.5 Hz), 125.5 (q, *J* = 3.5 Hz), 123.4 (q, *J* = 272.6 Hz), 123.0 (q, *J* = 272.8 Hz), 120.5 (dt, *J* = 7.6, 3.7 Hz), 113.9, 108.1. HR-ESMS calcd for $C_{20}H_9F_9NOS^-$ (M − H) 482.0267, found 482.0278.

(2-Amino-4-(3,5-bis(trifluoromethyl)phenyl)thiophen-3-yl)(4-tolyl)methanone (8g). Method B. Compound **8g** was isolated as a yellow solid (102 mg, 13%) after recrystallization from a mixture of 2-propanol, water, and acetone. ^{1}H NMR (400 MHz, CDCl₃) δ 7.45 (s, 1H), 7.40 (s, 2H), 7.14−7.08 (m, 2H), 6.77 (m, 4H), 6.28 (s, 1H), 2.15 (s, 3H). ^{13}C NMR (101 MHz, CDCl₃) δ 192.4, 166.3, 141.6, 139.6, 139.0, 137.1, 131.0 (q, *J* = 33.3 Hz), 128.8, 128.6 (d, *J* = 2.7 Hz), 128.4, 123.2 (q, *J* = 272.8 Hz), 119.9 (dt, *J* = 7.6, 3.8 Hz), 114.8, 107.4, 21.3. HR-ESMS calcd for $C_{20}H_{14}F_6NOS^+$ (M + H) 430.0695, found 430.0705.

(2-Amino-5-methyl-4-(3-(trifluoromethyl)phenyl)thiophen-3-yl)-(phenyl)methanone (8h). Method A. Compound **8h** was isolated as a yellow resin, which slowly solidified upon standing and was recrystallized from 2-propanol (587 mg, 66% yield); mp 129−131 °C. ^{1}H NMR (400 MHz, CDCl₃) δ 7.22−7.12 (m, 4H, ArH), 7.15−7.01 (m, 3H, ArH), 6.99−6.89 (m, 2H, ArH), 6.67 (bs, 2H, NH₂), 2.16 (s, 3H, CH₃). ^{13}C NMR (100 MHz, CDCl₃) δ 192.8, 164.0, 140.2, 137.3, 134.5, 133.3, 130.2, 129.9 (d, *J* = 32.1 Hz), 128.4, 128.1, 127.4, 127.1 (q, *J* = 3.7 Hz), 124.0 (q, *J* = 272.4 Hz), 123.0 (q, *J* = 3.5

Hz), 118.0, 116.1, 13.4. HR-ESMS calcd for $C_{19}H_{15}F_3NOS^+$ (M + H) 362.0821, found 362.0838.

(2-Amino-5-methyl-4-(3-(trifluoromethyl)phenyl)thiophen-3-yl)(4-chlorophenyl)methanone (8i). Method A. Compound **8i** was isolated as a yellow resin (342 mg, 35% yield). ^{1}H NMR (400 MHz, CDCl₃) δ 7.25 (d, *J* = 7.2 Hz, 1H, ArH), 7.21−6.97 (m, 5H, ArH), 6.96−6.82 (m, 2H, ArH), 6.44 (bs, 2H, NH₂), 2.15 (s, 3H, CH₃). ^{13}C NMR (101 MHz, CDCl₃) δ 191.3, 164.5, 138.6, 137.1, 136.2, 134.2, 133.3, 130.1 (q, *J* = 32.2 Hz), 129.7, 128.3, 127.6, 127.1 (q, *J* = 3.8 Hz), 123.9 (q, *J* = 272.5 Hz), 123.1 (q, *J* = 3.7 Hz), 118.2, 115.9, 13.4. HR-ESMS calcd for $C_{19}H_{14}ClF_3NOS^+$ (M + H) 396.0431, found 396.0439.

(2-Amino-5-methyl-4-(3-(trifluoromethyl)phenyl)thiophen-3-yl)-(3,4-dichlorophenyl)methanone (8j). Method B. Compound **8j** was isolated as an orange oil (137 mg, 25% yield). ^{1}H NMR (CDCl₃, 400 MHz) δ 7.28−7.21 (m, 2H), 7.15 (app d, *J* = 7.2, 1H), 7.10 (app t, *J* = 1.2, 2H), 7.06 (app d, *J* = 5.2, 2H), 6.83 (br s, 2H), 2.16 (s, 3H). ^{1}H NMR (400 MHz, CDCl₃) δ 7.29−7.20 (m, 2H), 7.18−7.14 (m, 1H), 7.12−7.09 (m, 2H), 7.05 (m, 2H), 6.84 (s, 2H), 2.16 (s, 3H). ^{13}C NMR (101 MHz, CDCl₃) δ 189.6, 165.1, 139.9, 137.1, 134.2, 134.0, 133.2, 131.5, 130.5, 130.3 (q, *J* = 32.5 Hz), 129.8, 128.5, 127.3, 126.8 (q, *J* = 3.8 Hz), 123.9 (q, *J* = 272.6 Hz), 123.3 (q, *J* = 3.7 Hz), 118.5, 115.6, 13.4. HR-ESMS calcd for $C_{19}H_{13}Cl_2F_3NOS^+$ (M + H) 430.0042, found 430.0059.

(2-Amino-5-methyl-4-(3-(trifluoromethyl)phenyl)thiophen-3-yl)(3-(trifluoromethyl)phenyl)methanone (8k). Method B. Compound **8k** was isolated as a yellow oil (123 mg, 24%). ^{1}H NMR (400 MHz, CDCl₃) δ 7.41 (d, *J* = 7.7 Hz, 1H), 7.35−7.28 (m, 2H), 7.19−7.08 (m, 5H), 6.88 (s, 2H), 2.16 (s, 3H). ^{13}C NMR (101 MHz, CDCl₃) δ 190.9, 165.1, 141.1, 136.9, 134.0, 133.3 (d, *J* = 1.1 Hz), 131.4 (d, *J* = 1.0 Hz), 130.2 (q, *J* = 32.3 Hz), 129.6 (q, *J* = 32.6 Hz), 128.5, 128.4, 126.9 (q, *J* = 3.8 Hz), 126.6 (q, *J* = 3.6 Hz), 125.1 (q, *J* = 3.6 Hz), 123.8 (q, *J* = 272.5 Hz), 123.7 (q, *J* = 272.5 Hz), 123.3 (q, *J* = 3.7 Hz), 118.5, 115.6, 13.4. HR-ESMS calcd for $C_{20}H_{14}F_6NOS^+$ (M + H) 430.0695, found 430.0714.

(2-Amino-5-methyl-4-(3-(trifluoromethyl)phenyl)thiophen-3-yl)(4-tolyl)methanone (8l). Method B. Compound **8l** was isolated as a yellow oil (36 mg, 5%). ^{1}H NMR (400 MHz, CDCl₃) δ 7.20−7.16 (m, 1H), 7.13 (s, 1H), 7.11−7.08 (m, 2H), 7.06 (d, *J* = 8.1 Hz, 2H), 6.72 (d, *J* = 7.8 Hz, 2H), 6.62 (s, 2H), 2.16 (s, 3H), 2.14 (s, 3H). ^{13}C NMR (101 MHz, CDCl₃) δ 192.9, 163.4, 140.6, 137.4 (d, *J* = 2.2 Hz), 134.7, 133.3, 129.8 (q, *J* = 32.2 Hz), 128.6, 128.1, 128.0, 127.1 (q, *J* = 3.8 Hz), 124.1 (q, *J* = 272.8 Hz), 122.7 (q, *J* = 3.7 Hz), 117.9, 116.5, 21.3, 13.4. HR-ESMS calcd for $C_{20}H_{17}F_3NOS^+$ (M + H) 376.0977, found 376.0975.

(2-Amino-4-(3,5-bis(trifluoromethyl)phenyl)-5-methylthiophen-3-yl)(phenyl)methanone (8m). Method B. Compound **8m** was isolated as a yellow gum (66 mg, 15%). ^{1}H NMR (400 MHz, CDCl₃) δ 7.41 (s, 1H), 7.34 (s, 2H), 7.15−7.10 (m, 2H), 7.09−7.03 (m, 1H), 6.98−6.91 (m, 2H), 6.79 (s, 2H), 2.16 (s, 3H). ^{13}C NMR (101 MHz, CDCl₃) δ 192.5, 164.4, 140.1, 138.7, 133.1, 130.9 (q, *J* = 33.3 Hz), 130.4, 130.2 (d, *J* = 2.6 Hz), 128.2, 127.7, 123.2 (q, *J* = 272.7 Hz), 120.0 (dt, *J* = 7.6, 3.7 Hz), 119.0, 115.6, 13.3. HR-ESMS calcd for $C_{20}H_{14}F_6NOS^+$ (M + H) 430.0695, found 430.0704.

(2-Amino-4-(3,5-bis(trifluoromethyl)phenyl)-5-methylthiophen-3-yl)(4-chlorophenyl)methanone (8n). Method B. Compound **8n** was isolated as an orange oil (151 mg, 26%). ^{1}H NMR (CDCl₃, 400 MHz) δ 7.51 (s, 1H), 7.33 (s, 2H), 7.08−7.02 (m, 2H), 6.94−6.88 (m, 2H), 6.83 (br s, 2H), 2.17 (s, 3H). ^{13}C NMR (101 MHz, CDCl₃) δ 191.0, 164.7, 138.6, 138.5, 136.6, 132.8, 131.2 (q, *J* = 33.3 Hz), 130.2 (d, *J* = 2.5 Hz), 129.6, 127.9, 123.1 (q, *J* = 272.8 Hz), 120.1 (dt, *J* = 7.4, 3.7 Hz), 119.2, 115.7, 13.3. HR-ESMS calcd for $C_{20}H_{13}ClF_6NOS^+$ (M + H) 464.0305, found 464.0304.

(2-Amino-4-(3,5-bis(trifluoromethyl)phenyl)-5-methylthiophen-3-yl)(3,4-dichlorophenyl)methanone (8o). Method B. Compound **8o** was isolated as an orange oil (160 mg, 25%). ^{1}H NMR (CDCl₃, 400 MHz) δ 7.53 (s, 1H), 7.36 (s, 2H), 7.11−7.01 (m, 3H), 6.92 (br s, 2H), 2.17 (s, 3H). ^{13}C NMR (101 MHz, CDCl₃) δ 189.3, 165.5, 139.8, 138.5, 134.6, 132.5, 131.9, 131.4 (q, *J* = 33.1 Hz), 130.3, 130.0, 129.9 (d, *J* = 2.7 Hz), 127.2, 123.1 (q, *J* = 272.7 Hz), 120.3 (dt, *J* = 7.5,

3.8 Hz), 119.6, 115.2, 13.4. HR-ESMS calcd for $C_{20}H_{12}Cl_2F_6NOS^+$ (M + H) 497.9915, found 497.9933.

(2-Amino-4-(3,5-bis(trifluoromethyl)phenyl)-5-methylthiophen-3-yl)(3-(trifluoromethyl)phenyl)methanone (8p). Method B. Compound **8p** was isolated as an orange oil (167 mg, 27%). ^{1}H NMR (CDCl$_3$, 400 MHz) δ 7.43−7.40 (m, 2H), 7.34−7.32 (m, 4H), 7.16 (t, J = 7.6, 1H), 6.92 (br s, 2H), 2.18 (s, 3H). ^{13}C NMR (101 MHz, CDCl$_3$) δ 190.4, 165.4, 141.0, 138.3, 132.5, 131.4 (d, J = 0.9 Hz), 131.3 (q, J = 33.3 Hz), 130.1 (q, J = 33.5 Hz), 130.0 (d, J = 2.7 Hz), 128.6, 126.9 (q, J = 3.6 Hz), 125.0 (q, J = 3.8 Hz), 123.5 (q, J = 272.5 Hz), 123.0 (q, J = 272.8 Hz), 120.3 (dt, J = 7.6, 3.7 Hz), 119.7, 115.3, 13.4. HR-ESMS calcd for $C_{21}H_{13}F_9NOS^+$ (M + H) 498.0569, found 498.0573.

(2-Amino-4-(3,5-bis(trifluoromethyl)phenyl)-5-methylthiophen-3-yl)((4-tolyl)methanone (8q). Method B. Compound **8q** was isolated as a yellow oil (121 mg, 22%). ^{1}H NMR (CDCl$_3$, 400 MHz) δ 7.42 (s, 1H), 7.32 (s, 2H), 7.01 (d, J = 7.9 Hz, 2H), 6.76−6.64 (m, 4H), 2.16 (s, 3H), 2.13 (s, 3H). ^{13}C NMR (101 MHz, CDCl$_3$) δ 192.6, 163.8, 140.8, 138.9, 137.3, 133.3, 130.9 (q, J = 33.2 Hz), 130.2 (d, J = 2.6 Hz), 128.4, 128.3, 123.2 (q, J = 272.6 Hz), 119.7 (dt, J = 7.7, 3.9 Hz), 118.9, 116.2, 21.2, 13.3. HR-ESMS calcd for $C_{21}H_{16}F_6NOS^+$ (M + H) 444.0851, found 444.0869.

Crystallography. Intensity data for the dimer of compound **8h** was collected with an Oxford Diffraction Sapphire CCD diffractometer using Cu Kα radiation (graphite crystal monochromator λ = 1.54184 Å). The temperature during data collection was maintained at 130.0(1) using an Oxford cooling device. Data were reduced and corrected for absorption.[30] The structures were solved by direct methods and difference Fourier synthesis.[31] Thermal ellipsoid plots were generated using the program ORTEP-3[32] integrated within the WINGX[33] suite of programs.

Crystal Data for the 8h dimer. $C_{38}H_{24}F_6N_2S_2$, M = 686.71, T = 130.0(1) K, λ = 1.54184, monoclinic, space group $P\overline{1}$, a = 8.4415(11), b = 13.141(2), c = 15.552(2) Å, a = 102.37(1)°, β = 99.43(1)°, γ = 106.33(1)°, V = 1570.2(4) Å^3, Z = 2, D_c = 1.452 mg M^{-3}, μ(Cu Kα) 2.128 mm^{-1}, $F(000)$ = 704, crystal size 0.34 × 0.10 × 0.02 mm^3, 9065 reflections measured, 5266 independent reflections (R_{int} = 0.082), the final R was 0.0581 $[I > 2\sigma(I)]$ and $wR(F^2)$ was 0.1485 (all data).

Biology. *Materials.* Dulbecco's modified Eagle's medium and hygromycin B were purchased from Invitrogen (Carlsbad, CA). Fetal bovine serum (FBS) was purchased from ThermoTrace (Melbourne, VIC, Australia). Adenosine deaminase, derived from calf intestine, was purchased from Roche (Basel, Switzerland). The Sure-Fire cellular ERK1/2 assay kits were a generous gift from TGR BioSciences (Adelaide, SA, Australia). AlphaScreen reagents for ERK1/2 and cAMP assays were from PerkinElmer Life and Analytical Sciences. All other reagents were purchased from Sigma-Aldrich (St. Louis, MO).

Cell Culture. Flp-In CHO cells stably expressing adenosine A$_1$ receptors (CHO A$_1$R) were cultured at 37 °C in 5% CO$_2$ in DMEM supplemented with 5% (v/v) FBS, 16 mM HEPES (Stewart et al., 2009).

Extracellular Signal-Regulated Kinase 1/2 Phosphorylation Assays. Initial ERK1/2 phosphorylation time course experiments were performed to determine the time at which ERK1/2 phosphorylation was maximal after stimulation by each ligand. Cells were seeded into transparent 96-well plates at 30000 cells per well and grown for over 8 h. Cells were then washed once with phosphate-buffered saline (PBS) and incubated in serum-free DMEM at 37 °C overnight to allow FBS-stimulated phosphorylated ERK1/2 levels to subside. Before stimulation, cells were treated with 1 U·mL^{-1} ADA for 30 min. Cells were then stimulated with allosteric modulator for 5 min prior to the addition of R-PIA for a further 5 min at 37 °C in 5% CO$_2$. For all experiments, 3% (v/v) FBS was used as a positive control, and vehicle controls were also performed. The reaction was terminated by removal of drugs and lysis of cells with 100 µL of SureFire lysis buffer (TGR Biosciences). The lysates were agitated for 1−2 min and were diluted at a ratio of 4:1 (v/v) lysate/Surefire activation buffer in a total volume of 50 µL. Under low-light conditions, a 1:240 (v/v) dilution of AlphaScreen beads/Surefire reaction buffer was prepared and this was

mixed with the activated lysate mixture in a ratio of 6:5 (v/v), respectively, in a 384-well opaque Optiplate. Plates were incubated in the dark at 37 °C for 1 h before the fluorescence signal was measured by use of a Fusion plate reader (PerkinElmer Life and Analytical Sciences) with standard AlphaScreen settings. Data were normalized to the maximal response elicited by 10 µM R-PIA.[21]

cAMP Accumulation Assay. CHO A$_1$R cells were plated into 96-well plates and cultured overnight at 37 °C in 5% CO$_2$. Cells were washed with PBS and cultured overnight in serum-free media. Thirty minutes before assaying, the culture medium was replaced with phenol red-free DMEM with 0.1% bovine serum albumin (BSA), 1 U·mL^{-1} ADA, and 500 µM 3-isobutyl-1-methylxanthine, and incubated at 37 °C in 5% CO$_2$. Cells were treated with 10 µM forskolin, R-PIA, and/or allosteric modulators and incubated for 30 min at 37 °C in 5% CO$_2$ as per the manufacturer's instructions. Medium was aspirated, and cells were lysed in lysis buffer (dH$_2$O, 0.3% Tween 20, 5 mM HEPES, 0.1% BSA). Lysates were transferred to a 384-well plate, and mixtures of lysis buffer/donor bead-conjugated anti-cAMP antibody and lysis buffer/biotinylated cAMP/acceptor bead-conjugated streptavidin were added to the lysates according to the PerkinElmer cAMP Alphascreen protocol. Plates were incubated in the dark at room temperature overnight before the fluorescence signal was measured by use of a Fusion plate reader (PerkinElmer Life and Analytical Sciences) by use of standard AlphaScreen settings. Data were normalized to the response elicited by 10 µM forskolin at the same time point.[21]

Data Analysis. Computerized nonlinear regression was performed using Prism 5.03 (GraphPad Software, San Diego, CA). For whole-cell functional ligand combination studies, the interaction between the orthosteric agonist R-PIA and the allosteric ligands **8h** and **8i** was fitted to the operational model of allosterism and agonism[15,28] to derive functional estimates of modulator affinity, intrinsic efficacy, and the composite cooperativity on affinity and efficacy together. Quantitative measures of functional selectivity between agonists for different signaling assays were estimated using an operational model of agonism.[24,25] This analysis yielded a value of τ_B/K_B for each allosteric agonist, which was then normalized to the τ_A/K_A value of R-PIA as follows: $\Delta Log(\tau_B/K_B) = Log(\tau_B/K_B)_{Allo} - Log(\tau_A/K_A)_{R\text{-}PIA}$. Subsequently, the actual bias of each allosteric agonist for the different signaling pathways was determined by statistically evaluating the $\Delta Log(\tau_B/K_B)$ values between the pathways. The ligand bias of an agonist for one pathway, j1, over another, j2, is given as: Bias = $10^{\Delta\Delta Log(\tau_B/K_B)_{j1-j2}}$ where $\Delta\Delta Log(\tau_B/K_B)_{j1-j2} = \Delta Log(\tau_B/K_B)_{j1} - \Delta Log(\tau_B/K_B)_{j2} = LogBF$. To account for the propagation of error associated with the determination of composite parameters, the following equation was used: Pooled SEM = $((SEM1)^2 + (SEM2)^2)^{1/2}$.

■ AUTHOR INFORMATION

Corresponding Author
*For P.J.S.: phone, +61 (0)3 9903 9542; E-mail, Peter.Scammells@monash.edu For A.C.: phone, +61 (0)3 9903 9067; E-mail, Arthur.Christopoulos@monash.edu

Notes
The authors declare no competing financial interest.

■ ACKNOWLEDGMENTS

ABBREVIATIONS USED

2A3BT, 2-amino-3-benzoylthiophenes; A_1R, A_1 adenosine receptor; GPCR, G protein-coupled receptor; ERK1/2, extracellular signal-regulated kinases 1 and 2; DMEM, Dulbecco's Modified Eagle Medium; FBS, fetal bovine serum; R-PIA, N^6-(R-phenylisopropyl)adenosine

REFERENCES

(1) Lagerström, M. C.; Schiöth, H. B. Structural diversity of G protein-coupled receptors and significance for drug discovery. *Nature Rev. Drug Discovery* **2008**, *7*, 339−357.

(2) Christopoulos, A.; Kenakin, T. G Protein-receptor coupling allosterism and complexing. *Pharmacol. Rev.* **2002**, *54*, 323−374.

(3) Christopoulos, A. Allosteric binding sites on cell-surface receptors: novel targets for drug discovery. *Nature Rev. Drug Discovery* **2002**, *1*, 198−210.

(4) May, L. T.; Leach, K.; Sexton, P. M.; Christopoulos, A. Allosteric modulation of G protein-coupled receptors. *Annu. Rev. Pharmacol. Toxicol.* **2007**, *47*, 1−51.

(5) Conn, J. P.; Christopoulos, A.; Lindsley, C. W. Allosteric modulation of GPCRs: a novel approach for the treatment of CNS disorders. *Nature Rev. Drug Discovery* **2009**, *8*, 41−54.

(6) Bruns, R. F.; Fergus, J. H. Allosteric enhancement of adenosine A_1 receptor binding and function by 2-amino-3-benzoylthiophenes. *Mol. Pharmacol.* **1990**, *38*, 939−949.

(7) Bruns, R. F.; Fergus, J. H.; Coughenour, L. L.; Courtland, G. G.; Pugsley, T. A.; Dodd, J. H.; Tinney, F. J. Structure−activity relationships for enhancement of adenosine A1 receptor binding by 2-amino-3-benzoylthiophenes. *Mol. Pharmacol.* **1990**, *38*, 950−958.

(8) van der Klein, P. A. M.; Kourounakis, A. P.; IJzerman, A. P. Allosteric Modulation of the Adenosine A_1 Receptor. Synthesis and Biological Evaluation of Novel 2-Amino-3-benzoylthiophenes as Allosteric Enhancers of Agonist Binding. *J. Med. Chem.* **1999**, *42*, 3629−3635.

(9) Baraldi, P. G.; Zaid, A. Z.; Lampronti, I.; Fruttarolo, F. F.; Pavani, M. G.; Tabrizi, M. A.; Shyrock, J. C. S.; Leung, E.; Romagnoli, R. Synthesis and biological effects of a new series of 2-amino-3-benzoylthiophenes as allosteric enhancers of A_1-adenosine receptor. *Bioorg. Med. Chem. Lett.* **2000**, *10*, 1953−1957.

(10) Figler, H.; Olsson, R. A.; Linden, J. Allosteric enhancers of A_1 adenosine receptors increase receptor-G protein coupling and counteract guanine nucleotide effects on agonist binding. *Mol. Pharmacol.* **2003**, *64*, 1557−1564.

(11) Lütjens, H.; Zickgraf, A.; Figler, H.; Linden, J.; Olsson, R. A.; Scammells, P. J. 2-Amino-3-benzoylthiophene Allosteric Enhancers of A_1 Adenosine Agonist Binding: New 3-, 4-, and 5-Modifications. *J. Med. Chem.* **2003**, *46*, 1870−1877.

(12) Nikolakopoulos, G.; Figler, H.; Linden, J.; Scammells, P. J. 2-Aminothiophene-3-carboxylates and carboxamides as adenosine A_1 receptor allosteric enhancers. *Bioorg. Med. Chem.* **2006**, *14*, 2358−2365.

(13) Aurelio, L.; Figler, H.; Flynn, B. L.; Linden, J.; Scammells, P. J. 5-Substituted 2-aminothiophenes as A1 adenosine receptor allosteric enhancers. *Bioorg. Med. Chem.* **2008**, *16*, 1319−1327.

(14) Aurelio, L.; Valant, C.; Figler, H.; Flynn, B. L.; Linden, J.; Sexton, P. M.; Christopoulos, A.; Scammells, P. J. 3- and 6-Substituted 2-amino-4,5,6,7-tetrahydrothieno[2,3-c]pyridines as A_1 adenosine receptor allosteric modulators and antagonists. *Bioorg. Med. Chem.* **2009**, *17*, 7353−7361.

(15) Aurelio, L.; Valant, C.; Flynn, B. L.; Sexton, P. M.; Christopoulos, A.; Scammells, P. J. Allosteric Modulators of the Adenosine A_1 Receptor: Synthesis and Pharmacological Evaluation of 4-Substituted 2-Amino-3-benzoylthiophenes. *J. Med. Chem.* **2009**, *52*, 4543−4547.

(16) Aurelio, L.; Valant, C.; Flynn, B. L.; Sexton, P. M.; White, J. M.; Christopoulos, A.; Scammells, P. J. Effects of Conformational Restriction of 2-Amino-3-benzoylthiophenes on A_1 Adenosine Receptor Modulation. *J. Med. Chem.* **2010**, *53*, 6550−6559.

(17) Aurelio, L.; Christopoulos, A.; Flynn, B. L.; Scammells, P. J.; Sexton, P. M.; Valant, C. The synthesis and biological evaluation of 2-amino-4,5,6,7,8,9-hexahydrocyclooctal[b]thiophenes as allosteric modulators of the A_1 adenosine receptor. *Bioorg. Med. Chem. Lett.* **2011**, *21*, 3704−3707.

(18) Urban, J. D.; Clarke, W. P.; von Zastrow, M.; Nichols, D. E.; Kobilka, B.; Weinstein, H.; Javitch, J. A.; Roth, B. L.; Christopoulos, A.; Sexton, P. M.; Miller, K. J.; Spedding, M.; Mailman, R. B. Functional selectivity and classical concepts of quantitative pharmacology. *J. Pharmacol. Exp. Ther.* **2007**, *320*, 1−13.

(19) Stallaert, W.; Christopoulos, A.; Bouvier, M. Ligand functional selectivity and quantitative pharmacology at G protein-coupled receptors. *Expert Opin. Drug Discovery* **2011**, *6*, 811−825.

(20) Bhattacharya, S.; Linden, J. The allosteric enhancer, PD 81,723, stabilizes human A_1 adenosine receptor coupling to G proteins. *Biochim. Biophys. Acta* **1995**, *1265*, 15−21.

(21) Valant, C.; Aurelio, L.; Urmaliya, V. B.; White, P.; Scammells, P. J.; Sexton, P. M.; Christopoulos, A. Delineating the mode of action of adenosine A1 receptor allosteric modulators. *Mol. Pharmacol.* **2010**, *78*, 444−455.

(22) Tranberg, C. E.; Zickgraf, A.; Giunta, B. N.; Lütjens, H.; Figler, H.; Falke, R.; Fleischer, H.; Linden, J.; Scammells, P. J.; Olsson, R. A. 2-Amino-3-aroyl-4,5-dimethylthiophenes: agonist allosteric enhancers at A_1 adenosine receptors. *J. Med. Chem.* **2002**, *45*, 382−389.

(23) Gregory, K. J.; Hall, N. E.; Tobin, A. B.; Sexton, P. M.; Christopoulos, A. Identification of Orthosteric and Allosteric Site Mutations in M2 Muscarinic Acetylcholine Receptors That Contribute to Ligand-Selective Signaling Bias. *J. Biol. Chem.* **2010**, *285*, 7459−7474.

(24) Koole, C.; Wootten, D.; Simms, J.; Valant, C.; Sridhar, R.; Woodman, O. L.; Miller, L. J.; Summers, R. J.; Christopoulos, A.; Sexton, P. M. Allosteric ligands of the glucagon-like peptide 1 receptor (GLP-1R) differentially modulate endogenous and exogenous peptide responses in a pathway-selective manner: implications for drug screening. *Mol. Pharmacol.* **2010**, *78*, 465−465.

(25) Evans, B. A.; Broxton, N.; Merlin, J.; Sato, M.; Hutchinson, D. S.; Christopoulos, A.; Summers, R. J. Quantification of functional selectivity at the human α1A-adrenoceptor. *Mol. Pharmacol.* **2011**, *79*, 298−307.

(26) Keov, P.; Sexton, P. M.; Christopoulos, A. Allosteric modulation of G protein-coupled receptors: a pharmacological perspective. *Neuropharmacology* **2011**, *60*, 24−35.

(27) Canals, M.; Lane, J. R.; Wen, A.; Scammells, P. J.; Sexton, P. M.; Christopoulos, A. A Monod−Wyman−Changeux Mechanism Can Explain G Protein-Coupled Receptor (GPCR) Allosteric Modulation. *J. Biol. Chem.* **2012**, *287*, 650−659.

(28) Leach, K.; Sexton, P. M.; Christopoulos, A. Allosteric GPCR modulators: taking advantage of permissive receptor pharmacology. *Trends Pharmacol. Sci.* **2007**, *28*, 382−389.

(29) Leach, K.; Valant, C.; Sexton, P. M.; Christopoulos, A. Measurement of ligand−G protein-coupled receptor interactions. In *G Protein-Coupled Receptors*; Poyner, D. R., Wheatley, M., Eds.; Wiley−Blackwell: Oxford, UK, 2010; pp 1−29.

(30) *CrysAlis CCD, Version 1.171.32.5 (release 08−05−2007 CrysAlis171.NET)*; Oxford Diffraction Ltd.: Yarnton, UK, 2007; (compiled May 8 2007,13:10:02).

(31) Sheldrick, G. M. A short history of SHELX. *Acta Crystallogr., Sect. A: Found. Crystallogr.* **2008**, *A64*, 112−122.

(32) Farrugia, L. J. ORTEP-3 for windows—a version of ORTEP-III with a graphical user interface (GUI). *J. Appl. Crystallogr.* **1997**, *30*, 565.

(33) Farrugia, L. J. WinGX suite for small-molecule single-crystal crystallography. *J. Appl. Crystallogr.* **1999**, *32*, 837−838.